17th Australasian Fluid Mechanics Conference
Auckland, New Zealand
5-9 December 2010

# Decay of MHD turbulence at low magnetic Reynolds number

**P. Burattini[1], O. Zikanov[2] and B. Knaepen[1]**

[1]Physique Statistique et des Plasmas
Université Libre de Bruxelles, B-1050 Brussels, Belgium

[2]Department of Mechanical Engineering
University of Michigan, Dearborn, MI 48128-1491, USA

## Abstract

We report a detailed numerical investigation of homogeneous decaying turbulence in an electrically conducting fluid in the presence of a uniform constant magnetic field. The asymptotic limit of low magnetic Reynolds number is assumed. Large-eddy simulations with the dynamic Smagorinsky model are performed in a computational box sufficiently large to minimise the effect of periodic boundary conditions. The initial microscale Reynolds number is about 170 and the magnetic interaction parameter $N$ varies between 0 and 50. We find that, except for a short period of time when $N$=50, the flow evolution is strongly influenced by nonlinearity and cannot be adequately described by any of the existing theoretical models [12, 1]. One particularly noteworthy result is the near equipartition between the rates of Joule and viscous dissipations of the kinetic energy observed at all values of $N$ during the late stages of the decay. Further, the velocity components parallel and perpendicular to the magnetic field decay at different rates, whose value depends on the strength of the magnetic field and the stage of the decay.

## Introduction

A particular case of homogeneous turbulence is characterised by directional anisotropy. This can be observed in an electrically conductive fluid flowing in the presence of a uniform external magnetic field $\mathbf{B}_0$. Practical examples include crystal growth in semiconductors, molten metals in metallurgy, and lithium cooling blankets for future fusion reactors. In these and other circumstances, the magnetic field induced by the electric currents in the liquid metal is negligible, in comparison to that imposed externally. The magnetic Reynolds number being small, the quasi-static approximation [13] can be used to simplify the expression of the Lorentz force. According to this approximation, the flow is characterised by two non-dimensional parameters: the hydrodynamic Reynolds number $Re$ and the magnetic interaction parameter $N$ (or alternatively the Hartmann number $Ha = (ReN)^{1/2}$). $N$ represents the ratio of the Lorentz force to inertia. Hereafter, the combination of low magnetic Reynolds number, uniform magnetic field, and quasi-static approximation are always assumed, when referring to MHD turbulence of liquid metals.

The understanding of decaying MHD turbulence remains incomplete. The paucity of detailed data on the decay properties of MHD turbulence is partly due to the anisotropy, which complicates the analytical treatment, and partly to the complexity of the experiments reproducing such a case. Progress was nonetheless made by Moffatt [12], who considered the early stages of the decay of the velocity fluctuations after sudden application of a magnetic field of large intensity (i.e. $N \gg 1$). His analysis assumed a linear regime and, therefore, was valid only for a short time after the application of $\mathbf{B}_0$, well before nonlinear interactions arise. Moffatt [12] showed that the magnetic field introduced an imbalance between the different velocity components: the kinetic energy of the velocity parallel to the magnetic field becomes twice that of the velocities in the perpendicular directions. He also showed that the Fourier modes of the fluctuating velocity were more effectively damped along the direction of the magnetic field. The prediction was made that the kinetic energy would decay according to the power-law $t^{-1/2}$ for times $t$ much smaller than one eddy turn-over time. Due to the linearity hypothesis, however, this temporal limitation precluded any prediction in the so-called 'initial period' of the decay.

Alemany et al. [1] carried out an in-depth investigation of MHD grid turbulence. Their case is the experimental analogue of the present simulations and therefore is described in some detail here. The set-up consisted of a biplane grid moving in one direction inside a column of still mercury. Such arrangement is equivalent to that in grid turbulence experiments, e.g. [5], with the difference that, in the latter, the grid is stationary and the fluid is moved by a fan. The mercury was immersed in a uniform magnetic field, parallel to the direction of grid motion. Different values of $\mathbf{B}_0$ were tested, with $N$ varying from 0.1 to 1.36. The velocity parallel to $\mathbf{B}_0$ was measured at several distances $x$ from the grid, ranging from 0 to 19 mesh sizes $M$. Alemany et al. [1] found that, following the application of the magnetic field, the decay exponent $m$ of the power-law $u'^2 \sim x^{-m}$ ($u'$ is the velocity fluctuation rms) increased to 1.7, from $m$=1 at $\mathbf{B}_0$=0. Furthermore, $m$ was almost independent of $N$. Remarkably, the effect of $\mathbf{B}_0$ on the decay was *opposite* to that found by Kolesnikov and Tsinober [9].

Regarding the decay of MHD turbulence at low $Re_m$, there is presently a gap between theoretical results and available experimental data: the first apply to large values of $R_\lambda$ (the Reynolds number based on the Taylor microscale) and $N$, while the second are limited to moderate values of both parameters. Further, the present linearised theory strictly refers to the early or final stages of the decay, while empirical data were taken in the initial decay. Numerical simulations are therefore essential to close the gap between different regimes and elucidate the behaviour of decaying MHD turbulence in its entirety. The aim of our work is to provide a detailed analysis of the decay of MHD turbulence. LES in a box with periodic boundaries are performed. Using a sufficiently large box, we minimise the effect of the boundary conditions and achieve a close approximation of homogeneous turbulence. Flows with moderate values of $R_\lambda$ and fairly large values of $N$ are obtained. Among other results, our study clarifies the apparent contradictions between the experimental observations of Kolesnikov and Tsinober [9] and the development of the anisotropy as predicted by the linear theory at large and small scales.

## Problem specification

The evolution of incompressible homogeneous MHD turbulence under the effect of a uniform, external magnetic field $\mathbf{B}_0$

of intensity $B_0$ and direction $x_3$ is described by Roberts [13]

$$\partial_t u_i + u_k \partial_k u_i = -\frac{1}{\rho}\partial_i p + \nu \partial_k^2 u_i - \frac{\sigma B_0^2}{\rho} \partial_k^{-2} \partial_3^2 u_i \quad (1)$$

$$\partial_i u_i = 0. \quad (2)$$

Here, $\mathbf{u} = (u_1, u_2, u_3)$ is the velocity, $p$ the sum of the kinematic and magnetic pressure, $\sigma$ the electrical conductivity, $\rho$ the fluid density, $\nu$ the kinematic viscosity, $\partial_k^{-2}$ the formal inverse of the Laplacian operator $\partial_k^2$. It is assumed that the initial flow field has zero mean velocity and shear. In (1), the rightmost term is the Lorentz force expressed via the quasi-static approximation. The evolution equation of the Reynolds stress tensor is derived from (1) by multiplication by $u_j$, space averaging, and symmetrization

$$\frac{\mathrm{d}}{\mathrm{d}t}\overline{u_j u_i} = -\frac{1}{\rho}\underbrace{\overline{p\left(\partial_i u_j + \partial_j u_i\right)}}_{P_{ij}} - \underbrace{2\nu\left(\overline{\partial_k u_j \partial_k u_i}\right)}_{\varepsilon_{\nu_{ij}}} - \underbrace{\frac{\sigma B_0^2}{\rho}\left(\overline{u_j \partial_k^{-2}\partial_3^2 u_i} + \overline{u_i \partial_k^{-2}\partial_3^2 u_j}\right)}_{\varepsilon_{J_{ij}}}. \quad (3)$$

Hereafter, summation is implied over the same index (unless otherwise stated), the overbar denotes averaging over the homogeneous directions, and the explicit time dependence is dropped most of the times. The three tensors $P_{ij}$, $\varepsilon_{\nu_{ij}}$, and $\varepsilon_{J_{ij}}$ represent the effect of the pressure-rate-of-strain correlation, viscous dissipation and Joule dissipation. The trace of (3) yields the equation for the turbulent kinetic energy $K = \overline{u_i u_i}/2$, i.e.

$$\frac{\mathrm{d}}{\mathrm{d}t}\underbrace{\frac{1}{2}\overline{u_i u_i}}_{K} = \underbrace{-\nu\left(\overline{\partial_k u_i \partial_k u_i}\right)}_{\varepsilon_\nu} \underbrace{-\frac{\sigma B_0^2}{\rho}\left(\overline{u_i \partial_k^{-2}\partial_3^2 u_i}\right)}_{\varepsilon_J}. \quad (4)$$

Thus, the temporal decay of $K$ is due to the Joule dissipation rate $\varepsilon_J$ and to the viscous dissipation rate $\varepsilon_\nu$. The latter can be equivalently expressed by

$$\varepsilon_\nu = 2\nu\overline{s_{ij}s_{ij}} = \frac{1}{2}\nu\overline{\left(\partial_j u_i + \partial_i u_j\right)^2}, \quad (5)$$

where $s_{ij} = 1/2\left(\partial_j u_i + \partial_i u_j\right)$ is the fluctuating rate-of-strain tensor.

The importance of the last term in (1) with respect to inertia is quantified by the magnetic interaction parameter

$$N = \frac{\sigma B_0^2}{\rho}\frac{L}{(2K/3)^{1/2}}, \quad (6)$$

where $L$ is the integral length scale. As in other works [15, 14, 3, 2], in (6) $L$ is estimated from the isotropic flow, before applying $\mathbf{B}_0$. The interaction parameter can also be expressed as the ratio

$$N = T/\tau \quad (7)$$

of the eddy turn-over time

$$T = \frac{L}{(2K/3)^{1/2}} \quad (8)$$

to the magnetic damping time

$$\tau = \frac{\rho}{\sigma B_0^2}. \quad (9)$$

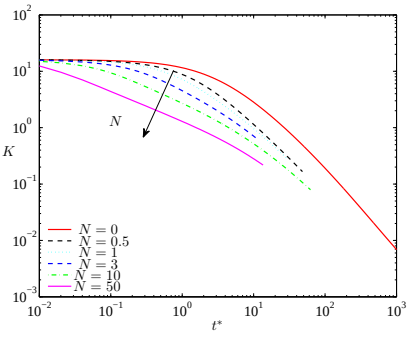


Figure 1: Decay of the turbulent kinetic energy at different values of the interaction parameter.

In the following, the asterisk indicates normalization of time by $T$.

### Numerical method

Equations (1)–(2) are solved in a domain with periodic boundary conditions using the LES approach. Details of the method are given in [7, 4] and only a brief description is provided here. The nonlinear term is evaluated in physical space while the other terms in Fourier space; aliasing errors are removed using the 2/3 algorithm. Time advancement is performed with a third-order, low-storage, Runge–Kutta integration scheme. The effect of the small scales on the resolved field is accounted via the Smagorinsky method using the dynamic procedure as modified by Lilly [10], in order to determine the volume-averaged Smagorinsky constant $C$ at each time step. In previous work [7, 15, 8], it was verified with the help of DNS data that the dynamic model accurately describes MHD turbulence. Under the quasi-static approximation, the Lorentz force is a linear function of the velocity and therefore commutes with the LES filtering. As a consequence, this approach does not require explicit modeling of the effect of the magnetic field on the subgrid-scale term.

### Results

Figure 1 reports the decay of $K$ at different values of $N$. For the hydrodynamic case, the profile is rather flat until, for $t^* \gtrsim 1$, viscous dissipation starts acting as the small scales are populated through the cascade. Compared to $N$=0, the primary effect of $\mathbf{B}_0$ is to shift the beginning of decay to an earlier time, especially at the largest values of $N$. This is due to the Joule dissipation, which acts immediately at all scales. Despite early differences, the distributions with $\mathbf{B}_0 \neq 0$ tend to converge at large times.

The available experiments in the literature reported the decay of either $K_\parallel$ or $K_\perp$. Figure 2 shows that, for any given value of $N$, the profile of $K_\parallel$ differs substantially from that of $K_\perp$. The relative importance of the two components of $K$ varies in time, with $K_\parallel$ and $K_\perp$ being the largest contributors of $K$ during respectively the early and late stages. This is illustrated by the inset of figure 2, which shows $K_\parallel/K_\perp$. The ratio is bounded from above by the value of 2. Such limit, which corresponds to the prediction of the linear model of [12], is attained only for $N = 50$, albeit briefly. It is worth noting that [11], who performed simulations of full MHD turbulence, showed that $K_\perp$ exceeds $K_\parallel$ at a late stage of the decay, although only for a compressible flow.

Some parts of the curves in figures 1 and 2 seemingly display a linear trend. This implies the establishment of a power-law of the type

$$K = (t - t_0)^{-m}, \quad (10)$$

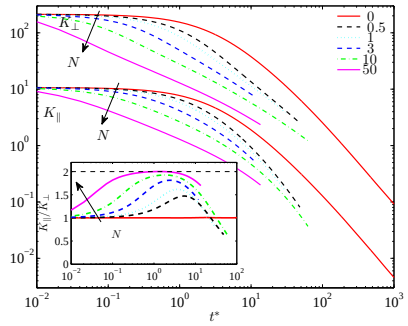


Figure 2: Decay of the turbulent kinetic energy of the parallel and perpendicular velocity components. Distributions of $K_\perp$ are shifted upwards by 20 units. Inset: ratios of the kinetic energy components.

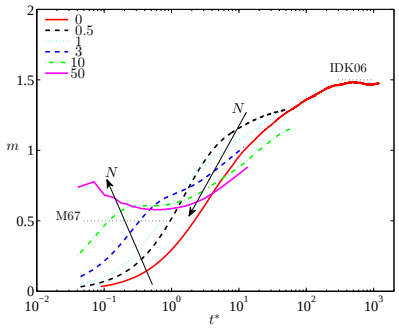


Figure 3: Logarithmic derivative of $K$. IDK06 ($m$=1.5) is the value computed by [6]; M67 (horizontal dashed line at $m$=1/2) is the value predicted by [12].

where $m(>0)$ is the decay exponent and $t_0$ the virtual origin. It should be stressed at the outset that, although such conclusion is supported by earlier experimental evidence ([1, 9]), it is not derivable analytically for intermediate values of $N$—that is, when both viscous and magnetic dissipation rates are not negligible. As remarked in the introduction, in the limit cases of $N \gg 1$ and $N \ll 1$ one can respectively use the linear theory of [12] with $m$=1/2 (but only for $\tau < t < T$) and the data collected for the pure hydrodynamic case.

The validity of (10) in our numerical experiment is verified directly by assuming $t \gg t_0$ and estimating the logarithmic derivative

$$m(t) = -\frac{\mathrm{d}\ln(K)}{\mathrm{d}\ln(t)} = -\frac{t}{K}\frac{\mathrm{d}K}{\mathrm{d}t}. \qquad (11)$$

If $K$ decays according to a power-law over a certain time interval, then the profile of $m(t)$ displays a plateau. This procedure is more reliable than fitting linearly a curve to the data over an arbitrary range. Distributions of $m$ computed via (11) are plotted in figure 3. After an early phase, the curve for $N$=0 levels off near 1.5. This value is in close agreement with that of [6], who performed DNS at high-resolution using, like here, an initial spectrum with a $k^4$ power-law at low wavenumbers. For the MHD cases, the decay rate is initially larger than in the hydrodynamic case. For $N$=10 and 50 and within one eddy turn-over time, $m$ displays a first plateau at $m \simeq 0.6$, slightly exceeding 1/2 of the linear theory. For lower values of $N$, the curves tend to level off only later and at larger values of $m$. At later stages, approximately for $t^* \gtrsim 1$ the decay rate decreases with increasing magnetic field.

As observed above, in any single previous experiment either $K_\parallel$ or $K_\perp$ was measured. Therefore, it is useful to examine the decay exponents $m_\parallel$ and $m_\perp$ of the individual velocity components. The results are presented in figures 4 and 5. For $N$=50, both sets of curves display the first plateau at $m \simeq 0.6$. As $N$ decreases, the regions of power-law of $K_\parallel$ disappear, while the power-law behaviour of $K_\perp$ becomes more evident at later times (estimates of $m_\perp$ in this regime are plotted in the inset of figure 4). From figures 4 and 5, one noteworthy observation can be made: at later times the decay rate of $K_\parallel$ is consistently larger than that of $K_\perp$. This inequality reconciles the observations of [1] and [9]. The first experiment provided $m_\parallel$=1.7 ($m$=1 at $N$=0) for $8 \leqslant x/M \leqslant 20$, while the second experiment $m_\perp$=0.23 ($m$=1.4 at $N \simeq 0$) for $2.5 \leqslant x/M \leqslant 40$ ([9]'s values have been estimated from their figures). While these values do not precisely match those calculated here, and admittedly $K_\parallel$ does not follow a power-law decay, our results nevertheless confirm that $K_\perp$ decays at a significantly slower rate than $K_\parallel$. This suggests that the differences between $m_\parallel$ and $m_\perp$ are intrinsic to this homogeneous flow, and that wall effects are not essential in order to explain the discrepancies between the two experiments, see also [4].

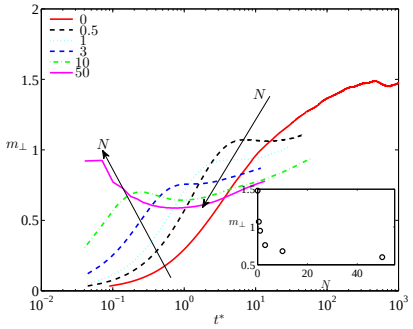


Figure 4: Logarithmic derivative of $K_\perp$. Inset: estimate of the decay exponents in the plateau region as a function of $N$.

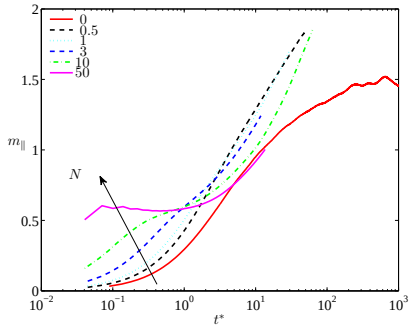


Figure 5: Logarithmic derivative of $K_\parallel$ .

Similarly to the other two terms of the kinetic energy budget (4), also $\varepsilon_J$ and more especially $\varepsilon_{J\perp}$ display a power-law (not shown). Accordingly, at later times the exponent $m_{J\perp}$ matches closely $m_{\nu\perp}$ and $(m_\perp + 1)$. This observation allows some general conclusions regarding the kinetic energy budget. At intermediate values of $N$ and large times, all three terms should be take into account in the kinetic energy budget of the perpendicular component, i.e.

$$\frac{\mathrm{d}}{\mathrm{d}t}K_\perp = -\varepsilon_{\nu\perp} - \varepsilon_{J\perp}. \qquad (12)$$

The power-law

$$K_\perp \sim t^{-m_\perp} \qquad (13)$$

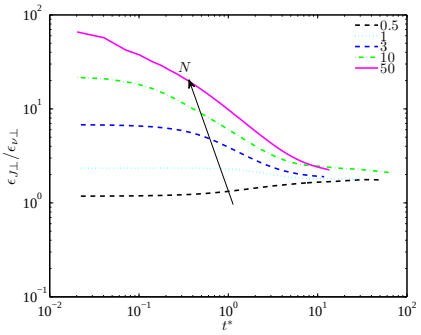


Figure 6: Ratio of Joule to viscous dissipation: perpendicular component.

is only possible if

$$\varepsilon_{J\perp} \sim t^{-m_\perp - 1} \quad (14)$$

$$\varepsilon_{\nu\perp} \sim t^{-m_\perp - 1}. \quad (15)$$

The last two relations imply that the ratio $\varepsilon_{J\perp}/\varepsilon_{\nu\perp}$ is constant. This can be verified directly from the numerical data, as illustrated by figure 6. For $t^* > 10$, the ratios converge towards a constant value, which, remarkably, is of order 1 for all the cases. Furthermore, also $\varepsilon_{J\parallel}$ and $\varepsilon_{\nu\parallel}$, and consequently $\varepsilon_J$ and $\varepsilon_\nu$ (not shown) display such equilibrium. By recognizing that the ratio $\varepsilon_J/\varepsilon_\nu$ has the form of the square of the Hartmann number $Ha$, one concludes that, within the time interval considered but irrespective of the value of $N$, the flow evolves towards a condition of $Ha$ of order unity. This represents an equipartition of the dissipations.

## Conclusions

The first conclusion of the present work is that the decay follows a complex path that cannot be fully described by any of the existing theoretical models. In particular, our simulations show that the linearised behaviour, which was earlier considered by [12] and computed by [14], is only followed for a short time. We find that the nonlinear effects rapidly dominate (after 1 eddy turn-over time) the flow evolution. As a consequence, the repartition of the kinetic energy between the velocity components quickly becomes the opposite of that suggested by the linear theory.

Regarding the establishment of the initial power-law for the decay of the kinetic energy, our results confirm the validity of the $t^{-1/2}$ decay. The data also show that later, in the nonlinear regime, the velocity components in the direction parallel and perpendicular to the magnetic field decay at different rates. This reconciles the apparent discrepancies between earlier experiments in grid turbulence.

As an entirely new and rather unexpected result, we observe that at the late stages of the decay, approximately after $10t^*$, the flow evolves into a state in which the viscous and Joule dissipation rates are nearly equal and only weakly sensitive to the strength of the magnetic field. The existence of such a 'nearly universal' state with equipartition between the viscous and Joule dissipation rates may serve as a basis for the development of theories of MHD turbulence decay.

## Acknowledgements

We acknowledge the support from the EURYI (European Young Investigator) Awards scheme (ESF), the Communauté Française de Belgique (ARC 02/07-283) and the EURATOM-Belgian state. The content of the publication is the sole responsibility of the authors and it does not necessarily represent the views of the Commission or its services.

## References

[1] Alemany, A., Moreau, R., Sulem, P. L. and Frisch, U., Influence of an external magnetic field on homogeneous MHD turbulence, *J. de Mécanique*, **18**, 1979, 277–313.

[2] Burattini, P., Kinet, M., Carati, D. and Knaepen, B., Anisotropy of velocity spectra in quasistatic magnetohydrodynamic turbulence, *Phys. Fluids*, **20**, 2008, 065110–1–065110–5.

[3] Burattini, P., Kinet, M., Carati, D. and Knaepen, B., Spectral energetics of quasi-static MHD turbulence, *Physica D*, **237**, 2008, 2062–2066.

[4] Burattini, P., Zikanov, O. and Knaepen, B., Decay of magnetohydrodynamic turbulence at low magnetic Reynolds number, *J. Fluid Mech.*, **657**, 2010, 502–538.

[5] Comte-Bellot, G. and Corrsin, S., Simple Eulerian time correlation of full- and narrow-band velocity signals in grid-generated, 'isotropic' turbulence, *J. Fluid Mech.*, **48**, 1971, 273–337.

[6] Ishida, T., Davidson, P. and Kaneda, Y., On the decay of isotropic turbulence, *J. Fluid Mech.*, **564**, 2006, 455–475.

[7] Knaepen, B., Kassinos, S. and Carati, D., Magnetohydrodynamic turbulence at moderate magnetic Reynolds number, *J. Fluid Mech.*, **513**, 2004, 199–220.

[8] Knaepen, B. and Moin, P., Large-eddy simulation of conductive flows at low magnetic Reynolds number, *Phys. Fluids*, **16**, 2004, 1255–1261.

[9] Kolesnikov, Y. and Tsinober, A., An experimental study of two-dimensional turbulence behind a grid, *Fluid Dyn.*, **9**, 1972, 621–624.

[10] Lilly, D. K., A proposed modification of the Germano subgrid-scale closure method, *Phys. Fluids*, **4**, 1992, 633–635.

[11] Matthaeus, W. H., Ghosh, S., Oughton, S. and Roberts, D. A., Anisotropic three-dimensional MHD turbulence, *J. Geophys. Res.*, **101**, 1996, 7619–7630.

[12] Moffatt, H. K., On the suppression of turbulence by a uniform magnetic field, *J. Fluid Mech.*, **28**, 1967, 571–592.

[13] Roberts, P. H., *An introduction to magnetohydrodynamics*, Elsevier, New York, 1967.

[14] Schumann, U., Numerical simulation of the transition from three- to two-dimensional turbulence under a uniform magnetic field, *J. Fluid Mech.*, **74**, 1976, 31–58.

[15] Vorobev, A., Zikanov, O., Davidson, P. A. and Knaepen, B., Anisotropy of magnetohydrodynamic turbulence at low magnetic Reynolds number, *Phys. Fluids*, **17**, 2005, 125105–1–125105–12.